PERGAMON

Chemical Engineering Science 55 (2000) 3275–3286

Chemical Engineering Science

Three-phase Eulerian simulations of bubble column reactors operating in the churn-turbulent regime: a scale up strategy

R. Krishna*, J. M. van Baten, M. I. Urseanu

Department of Chemical Engineering, University of Amsterdam, Nieuwe Achtergracht 166, 1018 WV Amsterdam, Netherlands

Received 25 May 1999; accepted 19 November 1999

Abstract

This paper develops a strategy for scaling up bubble column reactors operating in the churn-turbulent flow regime using computational fluid dynamics (CFD). The bubble column is considered to be made up of three phases: (1) liquid, (2) "small" bubbles and (3) "large" bubbles and the Eulerian description is used for each of these phases. Interactions between both bubble populations and the liquid are taken into account in terms of momentum exchange, or drag, coefficients, which differ for the "small" and "large" bubbles. The interactions between the large and small bubble phases are ignored. The turbulence in the liquid phase is described using the k–ε model. The three-phase description of bubble columns was implemented within the Eulerian framework of a commercial code CFX 4.2 of AEA Technology, Harwell, UK. Two types of approaches were first compared: (a) a simulation model assuming axi-symmetry and (b) a complete three-dimensional model for the cylindrical columns. The three-dimensional simulation showed chaotic behaviour. After averaging with respect to time and in the azimuthal direction, the radial distribution of liquid velocities corresponded closely with the two-dimensional axi-symmetric model. The total system gas hold-up predicted by these two simulation variants were also comparable though there was a significant difference in the radial distribution of the hold-up profiles of the large and small bubbles. For purposes of validation of the three-phase Eulerian simulation model, experiments were carried out in columns of 0.1, 0.174, 0.19, 0.38 and 0.63 m diameter. Three types of experiments were carried out: (1) dynamic gas disengagement experiments to determine the hold-ups of small and large bubble populations, (2) radial distribution of the axial component of the liquid velocity, and (3) centre-line liquid velocity. Demineralized water and Tellus oil, with a viscosity 75 times that of water, were used as liquid phase and air as gaseous phase. Comparison of the experimental measurements with the Eulerian simulations was used to conclude that the two-dimensional axi-symmetric model is adequate for scale up purposes. Simulations for columns with diameters ranging from 1 to 6 m were carried out to emphasise the strong influence of scale on the hydrodynamics.

Keywords: Bubble columns; Large bubbles; Small bubbles; Churn-turbulent flow regime; Bubble rise velocity; Radial velocity profiles; Column diameter influence; Computational fluid dynamics; Eulerian framework

1. Introduction

Bubble column reactors operated in industry have several distinguishing features: (1) large column diameters are involved, ranging to 6 m, (2) high superficial gas velocities, in the 0.1–0.4 m/s range, are usually used, (3) the system pressure can range to 6 MPa and (4) the liquid phase often consists of a non-aqueous hydrocarbon mixture (Krishna, Ellenberger & Sie, 1996). Laboratory studies on bubble column hydrodynamics are usually carried out with the air-water system, at ambient pressure conditions, in columns that are smaller than say 0.5 m in diameter (Deckwer, 1992). Even for the air–water system, available literature correlations give significantly different results. This is demonstrated by the predictions of the total gas hold-up and the centre-line liquid velocity as a function of the superficial gas velocity and column diameter; see Figs. 1 and 2. Only two correlations plotted in Fig. 1 anticipate that the gas hold-up decreases with increasing column diameter. We see from Fig. 2(b) that the predictions of the centre-line velocity for a bubble column of diameter 6 m diameter operating at $U = 0.3$ m/s varies between 0.9 and 4.5 m/s. This represents a variation of

* Corresponding author. Tel.: + 31-20-525-7007; fax + 31-20-525-5604.

E-mail address: krishna@chemeng.chem.uva.nl (R. Krishna)

0009-2509/00/$ - see front matter
PII: S0009-2509(99)00582-5

Nomenclature

AF	acceleration factor, m/s
d_b	diameter of either bubble population, m
C_D	drag coefficient, dimensionless
D_T	column diameter, m
$Eö$	Eötvös number, $g(\rho_L - \rho_G)d_b^2/\sigma$
g	acceleration due to gravity, 9.81 m/s^2
H	dispersion height, m
M	interphase momentum exchange term
p	pressure, N/m^2
r	radial coordinate, m
SF	scale correction factor, dimensionless
t	time, s
u	velocity vector, m/s
U	superficial gas velocity, m/s
V_b	rise velocity of bubble population, m/s
$V_L(r)$	radial distribution of liquid velocity, m/s
$V_L(0)$	centre-line liquid velocity, m/s

Greek letters

ε	volume fraction of gas phase, dimensionless
$\varepsilon(r)$	radial distribution of total gas hold-up, dimensionless
$\varepsilon(0)$	centre-line total gas hold-up, dimensionless
μ	viscosity of phase, Pa s
ρ	density of phases, kg/m^3
σ	surface tension of liquid phase, N/m
τ	stress tensor, N/m^2

Subscripts

b	referring to either bubble population
large	referring to the large bubble population
small	referring to the small bubble population
G	referring to gas phase
k	index referring to one of the three phases
L	referring to liquid phase
T	tower or column

a factor of five and so there is a clear need for a reliable scale up strategy.

The major objective of the present paper is to develop a model for predicting the scale dependence of the hydrodynamics of bubble column reactors operating in the churn-turbulent regime. The model is based on computational fluid dynamics (CFD) and uses an Eulerian description for the fluid phases. We attempt to validate, at least partially, the scale dependence predicted by the CFD model by comparison with experimental data generated in our laboratory in columns ranging in diameter from 0.1 to 0.63 m. Both experimental data from our data bank, partly published previously (Krishna & Ellenberger, 1996; Krishna, Urseanu, van Baten & Ellenberger, 1999b), and new experimental data generated in this work have been used for validation purposes. Furthermore, for purposes of validation of the CFD simulations we also use the experimental data on the radial distribution of gas hold-up and liquid velocity obtained by Hills (1974) in a 0.14 m diameter column with the air–water system.

2. Experimental

Two types of experiments were performed: (1) Dynamic gas disengagement experiments to determine the hold-ups of the "small" and "large" bubble populations

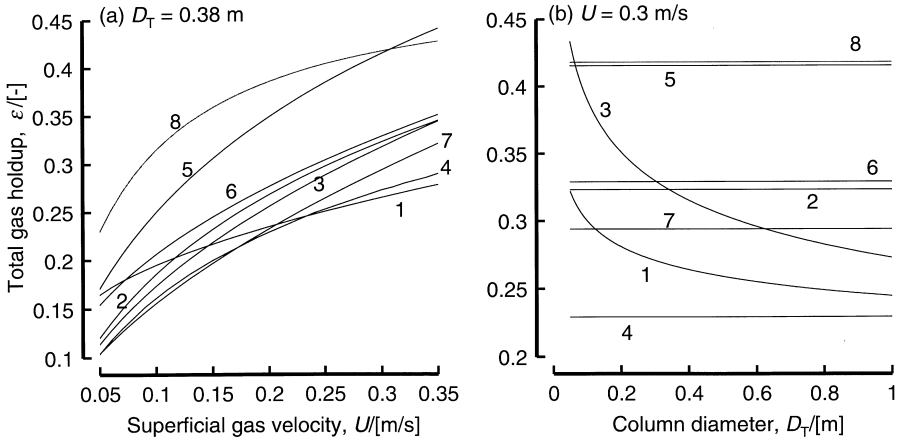

Fig. 1. Comparison of literature corrrelations for the total gas hold-up ε for air–water system in column of 0.38 m diameter: (a) Variation of ε with superficial gas velocity for a column of 0.38 m diameter; (b) Variation of ε with column diameter for a superficial gas velocity of 0.3 m/s. The plotted correlations are: (1) Krishna and Ellenberger (1996); (2) Wilkinson, Spek, and Van Dierendonck (1992); (3) Zehner (1986); (4) Akita and Yoshida (1973); (5) Bach and Pilhofer (1978); (6) Reilly, Scott, De Bruijn, Jain and Piskorz (1986); (7) Hikita, Asai, Tanigawa and Kitao (1980); (8) Hughmark (1967).

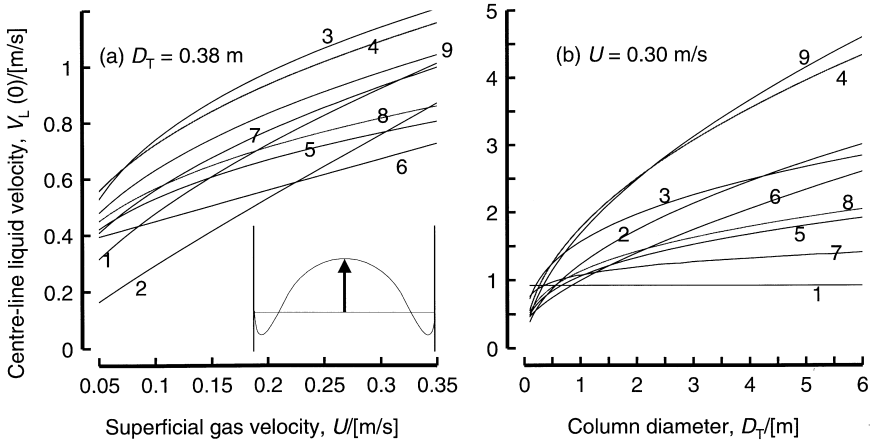

Fig. 2. Comparison of literature correlations for the centre-line velocity $V_L(0)$ for air–water system: (a) Variation of $V_L(0)$ with superficial gas velocity for a column of 0.38 m diameter; (b) Variation of $V_L(0)$ with column diameter for a superficial gas velocity of 0.3 m/s. The plotted correlations are: (1) Ohki and Inoue (1970); (2) Ueyama and Miyauchi (1979); (3) Joshi (1980); (4) Riquarts (1981); (5) Zehner (1986); (6) Nottenkämper, Steiff and Weinspach (1983); (7) Ulbrecht, Kawase and Auyeung (1985); (8) Kawase and Moo-Young (1989); (9) Bernemann (1989).

and (2) Measurement of the radial distribution of the axial component of the liquid velocity.

The description of the dynamic gas disengagement experiments data analysis procedure has been discussed earlier (Ellenberger & Krishna, 1994; Krishna & Ellenberger, 1996; Krishna, Van Baten & Ellenberger, 1998). For this study additional measurements were made to determine the total gas hold-up and the hold-ups of the "small" and "large" bubble populations for the system air–Tellus oil ($\mu_L = 0.075$; $\rho_L = 862$; $\sigma = 0.028$) in columns of 0.1, 0.19 and 0.38 m diameter.

The axial component of the liquid velocities along the radial positions at different superficial gas velocities were measured using a modified Pitot tube, also called "Pavlov tube" (Hills, 1974), in three columns with different inner diameters: 0.174, 0.38 and 0.63 m. All three columns were made up of four polyacrylate sections with the total height of 4 m. In all three columns the pressure at the top corresponded to ambient conditions (101.3 kPa). The 0.174 and 0.38 m diameter columns were equipped with sintered bronze plate gas distributors with an average pore size of 50 μm. The 0.63 m column was provided with a spider-shaped sparger, described in earlier work (Krishna & Ellenberger, 1996). The gas phase (air) was introduced at the bottom of the columns using different gas distributors. The liquid phase used in the experiments was either demineralised water or Tellus oil. A detailed description of the experimental set-ups, data analysis of the signals from the Pavlov tube, along with the underlying theory is available on our website: http://ct-cr4. chem.uva.nl/bc.

3. Development of CFD model

For the homogeneous regime of operation of bubble columns a more or less uniform bubble size is obtained (Clift, Grace & Weber, 1978). Many CFD approaches have been successfully developed to cater for this homogeneous regime of operation using the Eulerian description for the gas and liquid phases (Boisson & Malin, 1996; Grevskott, Sannæs, Dudukovic, Hjarbo & Svendsen, 1996; Grienberger & Hofmann, 1992; Jakobsen, Sannæs, Grevskott & Svendsen, 1997; Kumar, Vanderheyden, Devanathan, Padial, Dudukovic & Kashiwa, 1995; Lapin & Lübbert, 1994; Sanyal, Vasquez, Roy & Dudukovic, 1999; Sokolichin & Eigenberger, 1994; Sokolichin & Eigenberger, 1999; Torvik & Svendsen, 1990).

In the churn-turbulent regime of operation the bubble sizes vary over a wide range between 1 and 50 mm depending on the operating conditions and phase properties (De Swart, Van Vliet & Krishna, 1996). The rise characteristics of the bubbles depend on its size and liquid phase properties (Clift et al., 1978; Fan & Tsuchiya, 1990; Krishna & van Baten, 1999). Our approach for modelling purposes is to assume that in the churn-turbulent flow regime we have two distinct bubble classes: "small" and "large"; see Fig. 3. The small bubbles are in the size range of 1–6 mm and are either spherical or ellipsoidal in shape depending the physical properties of the liquid (Clift et al., 1978). The large bubbles are typically in the range of 20–80 mm range (De Swart et al., 1996) and fall into the spherical cap regime. These bubbles undergo frequent coalescence and break-up. The rise velocities of the large bubbles can approach 2 m/s and has been found to be significantly scale dependent (Krishna & Ellenberger, 1996) and because of the severe bypassing effect, these bubbles largely determine the gas phase conversion. In conformity with the Krishna–Ellenberger model, we assume that the superficial gas velocity through the small bubble phase corresponds to that at the regime transition point, U_{trans}. The transition

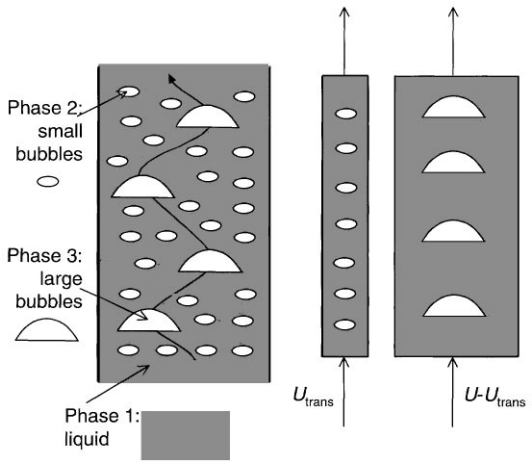

Fig. 3. Three-phase model for bubble columns operating in the churn-turbulent regime.

velocity can be estimated using the Reilly, Scott, De Bruijn and MacIntyre (1994) correlation or provided as model input.

For each of the three phases shown in Fig. 3 the volume-averaged mass and momentum conservation equations in the Eulerian framework are given by

$$\frac{\partial(\varepsilon_k \rho_k)}{\partial t} + \nabla\cdot(\rho_k \varepsilon_k \boldsymbol{u}_k) = 0, \tag{1}$$

$$\frac{\partial(\rho_k \varepsilon_k \mathbf{u}_k)}{\partial t} + \nabla\cdot(\rho_k \varepsilon_k \mathbf{u}_k \mathbf{u}_k - \mu_k \varepsilon_k (\nabla \mathbf{u}_k + (\nabla \mathbf{u}_k)^{\mathrm{T}})) = -\varepsilon_k \nabla p + \mathbf{M}_{kl} + \rho_k \mathbf{g}, \tag{2}$$

where ρ_k, $\mathbf{u}_k$, ε_k and μ_k represent, respectively, the macroscopic density, velocity, volume fraction and viscosity of the kth phase, p is the pressure, $\mathbf{M}_{kl}$, the interphase momentum exchange between phase k and phase l and $\mathbf{g}$ is the gravitational force.

The momentum exchange between either bubble phase (subscript b) and liquid phase (subscript L) phases is given by

$$\mathbf{M}_{L,b} = \frac{3}{4}\rho_L \frac{\varepsilon_b}{d_b} C_D(\mathbf{u}_b - \mathbf{u}_L)|\mathbf{u}_b - \mathbf{u}_L|. \tag{3}$$

The liquid phase exchanges momentum with both the "small" and "large" bubble phases. No interchange between the "small" and "large" bubble phases have been included in the present model and each of the dispersed bubble phases exchanges momentum only with the liquid phase. The neglect of the interactions between the small and large bubble populations is due to the conclusion reached by Vermeer and Krishna (1981). The interphase drag coefficient is calculated from equation

$$C_D = \frac{4}{3}\frac{\rho_L - \rho_G}{\rho_L} g d_b \frac{1}{V_b^2}, \tag{4}$$

where V_b is the rise velocity of the appropriate bubble population. We have only included the drag force contribution to $\mathbf{M}_{L,b}$, in keeping with the works of Sanyal et al. (1999) and Sokolichin and Eigenberger (1999). The added mass force has been ignored in the present analysis. The reason for this neglect is because the focus of the simulations and experiments in this work is on the churn-turbulent flow regime. The distinguishing feature of this regime is the existence of large fast-rising bubbles. These large bubbles do not have a closed wake and the concept of added mass is not applicable. The small bubbles on the other hand do have a closed wake. However, in the churn-turbulent flow regime these bubbles suffer strong recirculations, moving downwards near the wall region. Inclusion of the added mass contributions to the small bubbles led to severe convergence difficulties. The added mass contributions were therefore omitted. Lift forces are also ignored in the present analysis because of the uncertainty in assigning values of the lift coefficients to the small and large bubbles. For the large bubbles, for which $E\ddot{o} > 40$ holds, literature data suggest the use of a negative lift coefficient, whereas for small bubbles for which typically $E\ddot{o} = 2$, the lift coefficient is positive (Jakobsen et al., 1997).

For the continuous, liquid, phase, the turbulent contribution to the stress tensor is evaluated by means of $k-\varepsilon$ model, using standard single-phase parameters $C_\mu = 0.09$, $C_{1\varepsilon} = 1.44$, $C_{2\varepsilon} = 1.92$, $\sigma_k = 1$ and $\sigma_\varepsilon = 1.3$. The applicability of the k-ε model has been considered in detail by Sokolichin and Eigenberger (1999). No turbulence model is used for calculating the velocity fields inside the dispersed "small" and "large" bubble phases.

From visual observations of bubble column operations with the air–water system, the small bubbles were observed to be in the 3–6 mm size range. The rise velocity of air bubbles is practically independent of bubble diameter in this size range and the Harmathy (1960) equation for the rise velocity

$$V_{b,\mathrm{small}} = 1.53(\sigma g/\rho_L)^{0.25} \tag{5}$$

is used in the simulation model developed here. For the air–Tellus oil system, our dynamic gas disengagement experiments showed that the hold-up of the small bubble population was less than 2% and so we decided to ignore this presence of the small bubbles altogether in the CFD calculations. This neglect is achieved by setting $U_{\mathrm{trans}} = 0$. The hydrodynamics of air–Tellus oil system corresponds roughly to a situation in which large (spherical cap) bubbles rise through the column in a chain. For air–water system the holdup of the small bubbles is roughly half of the total bubble population and the choice of the model parameter U_{trans} determines the holdup of the small bubble population (Krishna & Ellenberger, 1996). The large bubble rise velocity was modelled using the approach developed by Krishna, Urseanu, van Baten and Ellenberger (1999a), which

introduces an acceleration factor AF into the Collins (1967) relation for the rise of a single spherical cap bubble:

$$V_{b,\mathrm{large}} = 0.71\sqrt{gd_{b,\mathrm{large}}}(SF)(AF). \quad (6)$$

The expressions developed by Krishna et al. (1999a) for the large bubble size and acceleration factor for air–water and air–Tellus oil systems are used in this work for estimation of the drag coefficient for the large bubble phase.

A commercial CFD package CFX 4.2 of AEA Technology, Harwell, UK, was used to solve the equations of continuity and momentum. This package is a finite volume solver, using body-fitted grids. The grids are non-staggered and all variables are evaluated at the cell centres. An improved version of the Rhie and Chow (1983) algorithm is used to calculate the velocity at the cell faces. The pressure-velocity coupling is obtained using the SIMPLEC algorithm (Van Doormal & Raithby, 1984). For the convective terms in Eqs. (1) and (2) hybrid differencing was used. A fully implicit backward differencing scheme was used for the time integration.

Simulations were carried out for air–water and air–Tellus oil systems for column diameters of 0.1, 0.14, 0.174, 0.38, 0.63, 1, 2, 3, 4 and 6 m, operating at superficial gas velocities in the range $U = 0.019$ to 0.35 m/s. Details of the column configurations and the grids used are specified in Table 1. The air–Tellus oil system was modelled as consisting of two phases: large bubbles and liquid, which corresponded closely with our experimental observations. From the Reilly et al. (1994) correlation it was determined that the superficial gas velocity at the regime transition point for air–water $U_{\mathrm{trans}} = 0.034$ m/s. For air–water operation at $U < 0.034$ m/s, homogeneous bubbly flow regime was taken to prevail. Therefore, only two phases, small bubbles and liquid are present. For churn-turbulent operation at $U > 0.034$ m/s, the complete three phase model was invoked. Following the model of Krishna and Ellenberger (1996) we assume that in the churn-turbulent flow regime the superficial gas velocity through the small bubble phase is $U_{\mathrm{trans}} = 0.034$ m/s (see Fig. 3). The rest of the gas $(U - U_{\mathrm{trans}})$ was taken to rise up the column in the form of large bubbles. This implies that at the distributor the "large" bubbles constitute a fraction $(U - U_{\mathrm{trans}})/U$ of the total incoming volumetric flow, whereas the "small" bubble constitute a fraction (U_{trans}/U) of the total incoming flow. Strictly speaking, U_{trans} is a model parameter and its choice has a significant increasing effect on the small bubble holdup but its influence on the the centreline velocity is negligible (Krishna et al., 1999b). A further assumption made is that the formation of the large bubbles takes place immediately at the distributor; this is essentially a simplification and the justification for this is that our experimental studies show that the "large" bubbles equilibrate within a distance of 0.1 m above the distributor (Ellenberger & Krishna, 1994). The diameter of the "small" bubbles was chosen to be 4 mm in all the simulations for the air–water system and the drag coefficient determined from Eqs. (4) and (5). The large bubble drag coefficient was determined from Eqs. (4) and (6) using the expressions developed by Krishna et al. (1999a) for SF, AF and d_{b} for air-water and air-Tellus oil systems. The large bubbles were injected in the central core of the column because this is in conformity with visual observations. The small bubbles were distributed uniformly over the whole column with the exception of the wall region.

Most of the simulations were carried out using cylindrical axi-symmetry. The time stepping strategy used in the transient simulations for attainment of steady state was typically: 20 steps at 5×10^{-4} s, 20 steps at 1×10^{-3} s, 460 steps at 5×10^{-3} s, 2000 steps at 2×10^{-2} s. The 0.14, 0.174, 0.38 and 0.63 m diameter column simulations were carried out on a Silicon Graphics Power Indigo workstation with the R8000 processor. Each simulation was completed in about 36 h. In all the runs steady state was reached within 2500 time steps. Simulations of the 2, 4 and 6 m diameter columns were carried out on a Power Challenge machine employing three R10000 processors in parallel.

A number of fully three-dimensional simulations were also carried out for the 0.14, 0.174, 0.38 and 0.63 m diameter columns. The simulation of the 0.38 m diameter column operating at a superficial gas velocity of 0.23 m/s, involving 96000 grid cells, for example was carried out using the time stepping strategy: 100 steps at 5×10^{-4} s, 100 steps at 1×10^{-3} s, 9800 steps at 5×10^{-3} s. Running on a Silicon Graphics Power Challenge machine employing three R10000 processors in parallel, this simulation took 26 days to complete 10000 time steps.

Further details of the 2D and 3D simulations, including animations of column start-up dynamics are available on our web sites: http://ct-cr4.chem.uva.nl/euler2D and http://ct-cr4.chem.uva.nl/euler3D. A comparison of the 2D and 3D animations for 0.38 m diameter column operating at $U = 0.23$ m/s is available on our web site: http://ct-cr4.chem.uva.nl/oil-water.

4. Simulations vs. experiments

We first compare the results of two-dimensional axi-symmetric simulation with a complete three-dimensional simulation of a 0.38 m diameter column at $U = 0.23$ m/s with the air–water system. Fig. 4(a) shows the transient approach to steady state in the 2D simulation. The parameter values at the end of the simulation were taken to be the steady-state values. The corresponding 3D simulation shows chaotic behaviour (cf. Fig. 4(b) and (c)), which can best be appreciated by viewing the animations on our

Table 1
Column configurations, systems, operating conditions and grid details of CFD simulations

Liquid phase	Column diameter D_T/(m)	Column height/(m)	Initial liquid height/(m)	Observation height/(m)	Number of grid cells (radial) × (axial) × (azimuthal)	Superficial gas velocity, U/(m/s)	U_{trans}/(m/s)	2D/3D
Water	0.14	1.3	0.9	0.6	30 × 150	0.019, 0.038, 0.064, 0.095, 0.169	0.034	2D
Water	0.14	1.3	0.9	0.6	30 × 150 × 10	0.019, 0.038, 0.064, 0.095, 0.169	0.034	3D
Water	0.14	1.3	0.9	0.6	30 × 150 × 20	0.169	0.034	3D
Water	0.174	3	1.8, 2	1.6	30 × 160	0.02, 0.034, 0.09, 0.16, 0.23, 0.27, 0.3	0.034	2D
Water	0.174	3	1.8	1.6	30 × 160 × 20	0.23	0.034	3D
Water	0.38	3	1.8, 2	1.6	30 × 160	0.02, 0.034, 0.09, 0.16, 0.23, 0.285, 0.3, 0.35	0.034	2D
Water	0.38	3	1.8	1.6	30 × 160 × 20	0.23, 0.285, 0.3	0.034	3D
Water	0.63	3	1.8, 2	1.6	30 × 160	0.02, 0.034, 0.09, 0.16, 0.23, 0.27, 0.285, 0.3, 0.35	0.034	2D
Water	0.63	3	1.8	1.6	30 × 160 × 20	0.23, 0.285, 0.3	0.034	3D
Water	1	7	4	4	75 × 150	0.3	0.034	2D
Water	1.5	8	4.8	4.8	75 × 410	0.3	0.034	2D
Water	2	13,12	10, 7	9, 7	75 × 270	0.16, 0.3	0.034	2D
Water	3	15	10	10	75 × 310	0.3	0.034	2D
Water	4	25	20	18	75 × 510	0.16, 0.3	0.034	2D
Water	6	35	25, 20	18	75 × 710	0.16, 0.3	0.034	2D
Tellus oil	0.1	2	1.4	1.4	30 × 110	0.05, 0.09, 0.125, 0.16	0	2D
Tellus oil	0.19	2	1.4	1.4	30 × 110	0.05, 0.09, 0.16, 0.23, 0.3, 0.35	0	2D
Tellus oil	0.38	2	1.4	1.4	30 × 110	0.05, 0.09, 0.125, 0.16, 0.23, 0.3, 0.35	0	2D
Tellus oil	1.5	8	5.3	4.5	75 × 410	0.05, 0.09, 0.16	0	2D
Tellus oil	2	13	10	9	75 × 270	0.16, 0.3	0	2D
Tellus oil	4	25	20	20	75 × 510	0.16, 0.3	0	2D
Tellus oil	6	35	20	20	75 × 710	0.16, 0.3	0	2D

For operation at $U < U_{trans}$, homogeneous bubbly flow regime was taken to prevail. For operation at $U > U_{trans}$, the complete three phase model was invoked. The large bubble phase was injected over the central 13 (or 32) of the 30 (or 75) grid cells. The small bubble phase was injected over the central 24 (or 61) of the 30 (or 75) grid cells.The reported liquid velocity profiles are at the observation heights reported below. The reported values of the total gas holdup refer to the fractional gas volume below this observation height.

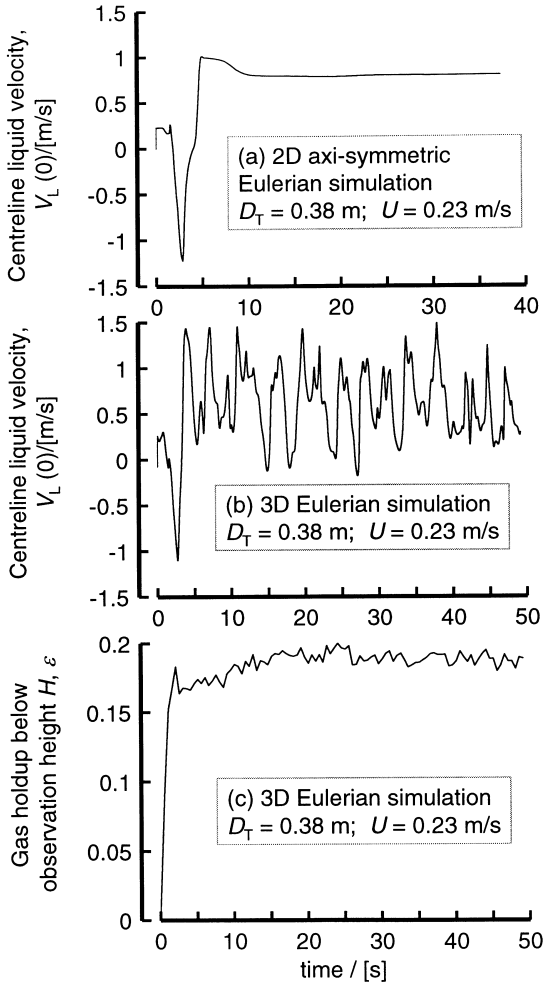

Fig. 4. Transient approach to steady state in CFD simulations of a 0.38 m diameter column with the air–water system operating at a superficial gas velocity of 0.23 m/s. The input parameters used in these simulations are: $U_{trans} = 0.034$ m/s; $d_{b,small} = 0.004$ m; $CD_{small} = 0.839$; $d_{b,large} = 0.037$ m; $CD_{large} = 0.204$: (a) The centre-line liquid velocity $V_L(0)$, monitored at 1.6 m above the distributor is plotted against time for the 2D axi-symmetric simulation with time stepping strategy: 20 steps at 5×10^{-4} s, 20 steps at 1×10^{-3} s, 460 steps at 5×10^{-3} s, 2000 steps at 2×10^{-2} s, (b) and (c) Three-dimensional simulation with time stepping strategy: 100 steps at 5×10^{-4} s, 100 steps at 1×10^{-3} s, 9800 steps at 5×10^{-3} s. Animations of the column start-up dynamics for the 2D and 3D simulations can be viewed on our web site: http://ct-cr4.chem.uva.nl/oil-water.

web site. http://ct-cr4.chem.uva.nl/oil-water. Fig. 5 shows snapshots of the liquid velocity vectors at a height 1.6 m above the distributor for three time steps. It is interesting to note that the azimuthal liquid motion switches direction chaotically. For comparison of 2D and 3D results the transient 3D data for hold-ups and velocities were time averaged (using the last 2000 time steps) and spatially averaged in the azimuthal direction.

The radial distribution of gas hold-up obtained with 2D and 3D simulations are compared in Fig. 6(a)–(e) with experimental data of Hills (1974) obtained in a 0.14 m diameter column. We note that the assumption of cylindrical axi-symmetry prevents lateral motion of the dispersed bubble phases and leads to an unrealistic gas bubble hold-up distribution wherein a maximum hold-up is experienced away from the central axis. In the 3D simulations, on the other hand, in which lateral motion in both radial and azimuthal directions are catered for (cf. Fig. 5), yield physically realistic distribution of gas hold-ups, and are in reasonably good agreement with experiment. Recent work of Bauer and Eigenberger (1999) have underlined the impact of lateral fluxes of mass and momentum, resulting from 3D simulations, in the proper simulation of tracer dispersion.

Fig. 7(a) compares the gas hold-up averaged over the cross-section at a height of 0.6 m above the distributor, from the simulations with the experimental values of Hills (1974). We see that though the 2D axi-symmetric simulation predicts an unrealistic radial distribution of gas hold-up, there is practically no difference between the 2D and 3D simulation results with respect to cross-section averaged hold-ups. The agreement with the experimental data of Hills (1974) is reasonable, though the simulations tend to systematically under-predict the gas hold-up. In order to emphasise the need for the including both "large" and "small" bubbles, we carried out simulations of the Hills experiments in which the "large" bubbles were ignored, i.e. assuming that the dispersion was made up only of small bubbles. The simulated values of the gas hold-up are seen to be extremely high, at variance with the experiments; see Fig. 7(a). The cumulative values of the gas hold-ups (large + small) are plotted in Fig. 7(b) as a function of the height above the distributor of a 0.38 m diameter column operating at $U = 0.3$ m/s. The cumulative gas hold-up values of the 2D and 3D simulations do not differ significantly and for a dispersion height of 1.6 m these values agree well with the experimentally determined value.

Fig. 8 compares the radial distribution of the axial component of the liquid velocity, normalized with respect to the centre-line velocity, $V_L(0)$, obtained from the 2D and 3D simulations with experiments in columns of 0.14, 0.38 m and 0.63 m in diameter. In Fig. 8(a)–(e) the two types of simulations are compared with the experimental data of Hills (1974). We see that both simulated profiles are close to each other and are able to reproduce the experimental trends very well. For the larger diameter columns, 0.38 and 0.63 m in diameter, operating at higher superficial gas velocity ($U = 0.285$ m/s) there are differences in the 2D and 3D simulated profiles of liquid velocity; see Figs. 8(i) and (j). The experimental data obtained in this work show that the 3D simulations have a better predictive character, as might be expected. The value of the centre-line liquid velocity predicted by the 2D and 3D simulations, monitored at a height 1.6 m above the distributor, are however close to each other.

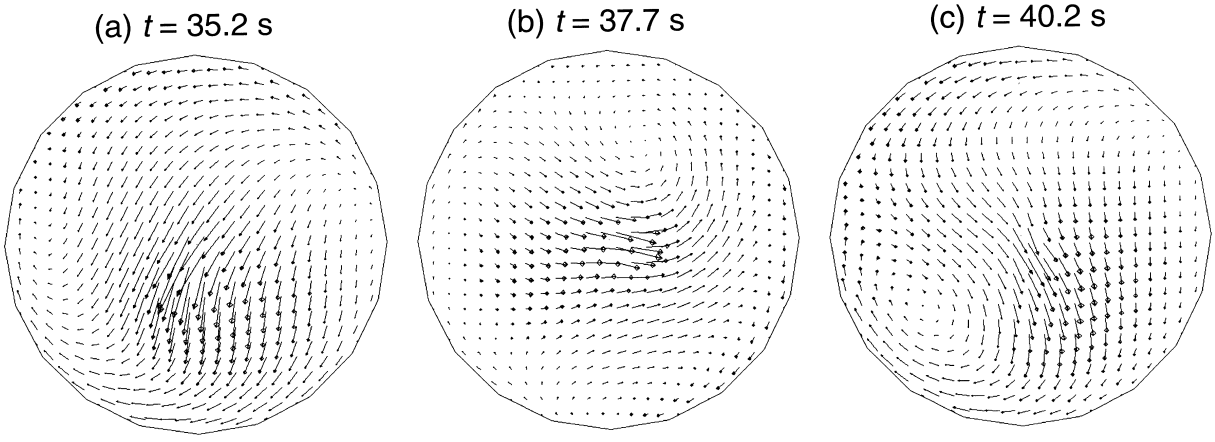

Fig. 5. Snapshots of the liquid velocity vectors at a height 1.6 m above the distributor for three time steps for the 3D simulation of a 0.38 m diameter column with the air–water system operating at a superficial gas velocity of 0.23 m/s. Animations of the column start-up dynamics for the 2D and 3D simulations can be viewed on our web site: http://ct-cr4.chem.uva.nl/oil-water.

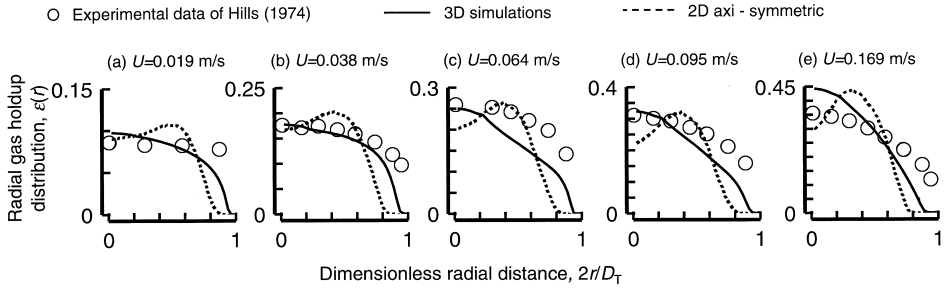

Fig. 6. Comparison of radial profiles of gas holdup obtained from 2D and 3D simulations of a 0.14 m diameter column for air–water system with experimental data of Hills (1974). Animations of the 2D and 3D simulations of can our web sites: http://ct-cr4.chem.uva.nl/euler2D and http://ct-cr4.chem.uva.nl/euler3D.

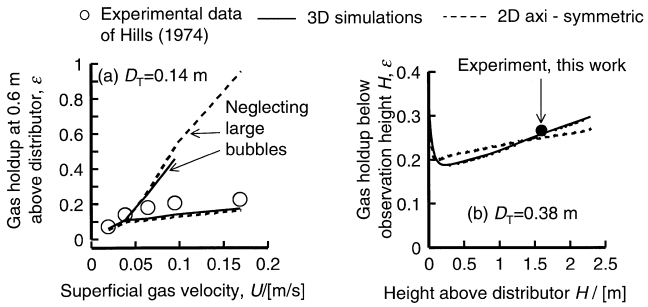

Fig. 7. (a) Comparison of gas hold-ups obtained from 2D and 3D simulations of a 0.14 m diameter column with air–water system with experimental data of Hills (1974). Also shown are simulation results in which the dispersion is assumed to consist only of small bubbles. The gas hold-up value corresponds to the average at a height of 0.6 m above the distributor; (b) Cumulative gas hold-up for a 0.38 m diameter column operating at a superficial gas velocity of 0.3 m/s. The 2D and 3D simulation results are compared with each other. Also indicated in the figure is the experimentally measured value below a dispersion height of 1.6 m.

For example for the 0.38 m column operating at $U = 0.3$ m/s, $V_L(0) = 0.88$ and 0.89 m/s for the 2D and 3D simulations, respectively.

We conclude from the results in Figs. 6–8 that a complete 3D simulation is required for accurate representation of the radial distributions of gas hold-ups and liquid velocities. However, if one is interested in cumulative gas hold-ups and centre-line velocities, a 2D simulation would be adequately accurate, as will be seen by comparing 2D simulation results with experimental data for air–water and air–Tellus oil systems; see Figs. 9 and 10. Fig. 9 shows that the gas hold-up is predicted adequately accurately for both air–water and air–Tellus oil systems. The predictions of $V_L(0)$ from Eulerian simulations reflect the strong column diameter dependence, observed experimentally. For the highly viscous Tellus oil as liquid phase the predictions of $V_L(0)$ CFD simulations are much closer to experimentally determined values than those of empirical correlations, e.g. due to Riquarts (1981)

$$V_L(0) = 0.21(gD_T)^{1/2}(U^3/g\nu_L)^{1/8} \tag{7}$$

and Zehner (1986):

$$V_L(0) = 0.737(U\ g\ D_T)^{1/3}. \tag{8}$$

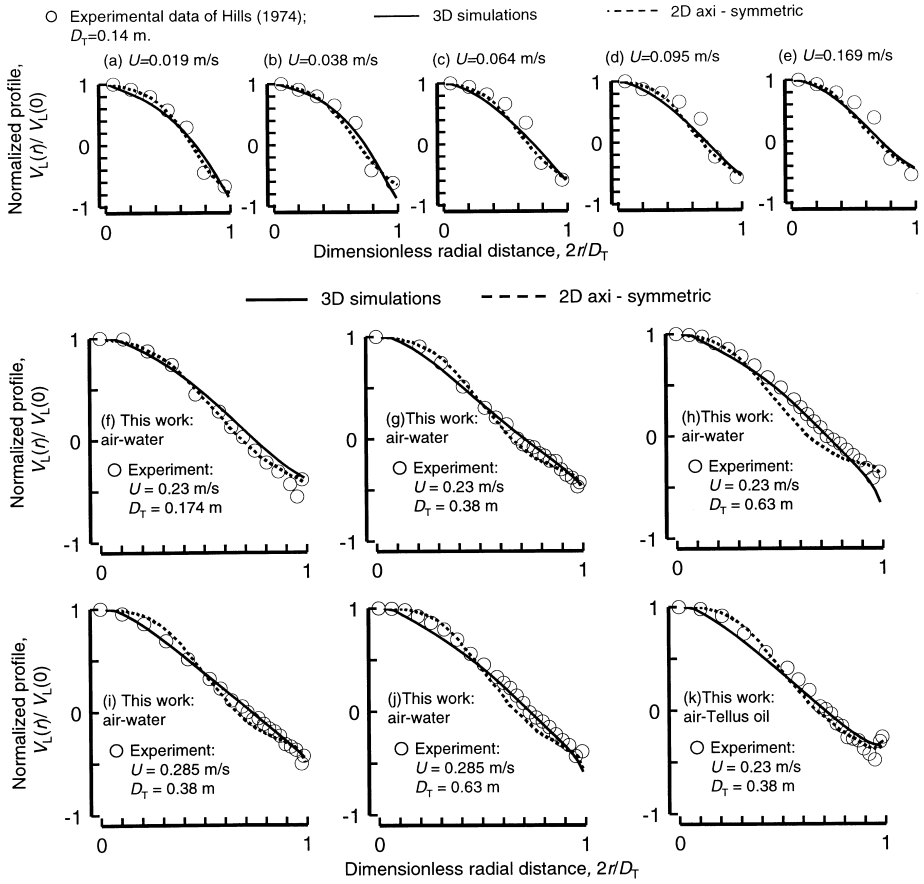

Fig. 8. Comparison of radial profiles of liquid velocity obtained from 2D and 3D simulations with experimental data with air–water system. (a)–(e) Comparison of simulations with experimental data in a 0.14 m diameter column used in the experiments of Hills (1974); (f)–(k) Comparison of simulations with experimental data generated in this work.

Interestingly, the correlation of Riquarts (1981) predicts a significantly lowering of $V_L(0)$ when the liquid viscosity is increased by a factor of 75, as is the case when we switch from water to Tellus oil. Our experiments in the 0.38 m diameter column with water (Fig. 10(b)) and Tellus oil (Fig. 10(f)), show very little influence of liquid viscosity on $V_L(0)$. The Eulerian simulations of $V_L(0)$ for water and Tellus oil systems give practically the same results for $V_L(0)$ over the superficial gas velocity range of 0.05–0.35 m/s, in broad agreement with experiment.

For a superficial gas velocities of 0.16 and 0.3 m/s, Eulerian simulations were carried out to study the influence of column diameter. The results for air–water and air–Tellus oil are shown in Fig. 11. In all simulations the column configurations and initial liquid heights were chosen such that the ratio of the dispersion height to the column diameter was about five; see Table 1. For air–water system the predictions of $V_L(0)$ agree remarkably well with that of Riquarts (1981) and demonstrate extremely strong scale dependence. The Riquarts correlation significantly underpredicts the values of $V_L(0)$ for the Tellus–oil system. Comparison of the simulations of $V_L(0)$ for air–water and air–Tellus oil shows that the centre-line velocity is practically independent of the liquid viscosity. Therefore, the Riquarts correlation (7) also works for air–Tellus oil provided we use the kinematic viscosity of water. Due to the strong circulations with increasing column diameter, the bubbles will be accelerated. This acceleration effect causes a significant reduction in the large bubble hold-up with increasing column diameter; see Figs. 11(a)–(d). Also shown are the calculations of the large bubble hold-up using the correlation of Krishna and Ellenberger (1996)

$$\varepsilon_{b,large} = 0.268 \frac{1}{D_T^{0.18}} \frac{1}{(U - U_{trans})^{0.22}} (U - U_{trans})^{4/5}, \tag{9}$$

where we have used $U_{trans} = 0$ for air–Tellus oil system. The decrease in the large bubble hold-up with column diameter from the Eulerian simulations is stronger than anticipated by Eq. (9), due to the significant increase in the liquid circulation velocity with increasing column diameter.

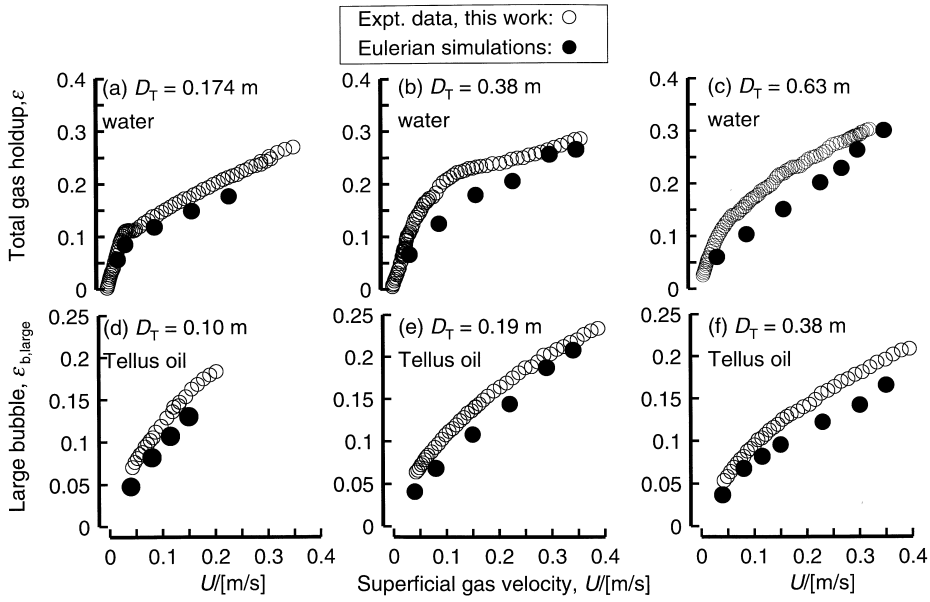

Fig. 9. Comparison of experimental values of gas hold-up with 2D Eulerian simulations. The simulated values of the gas hold-up are cumulative values below 1.6 m dispersion height.

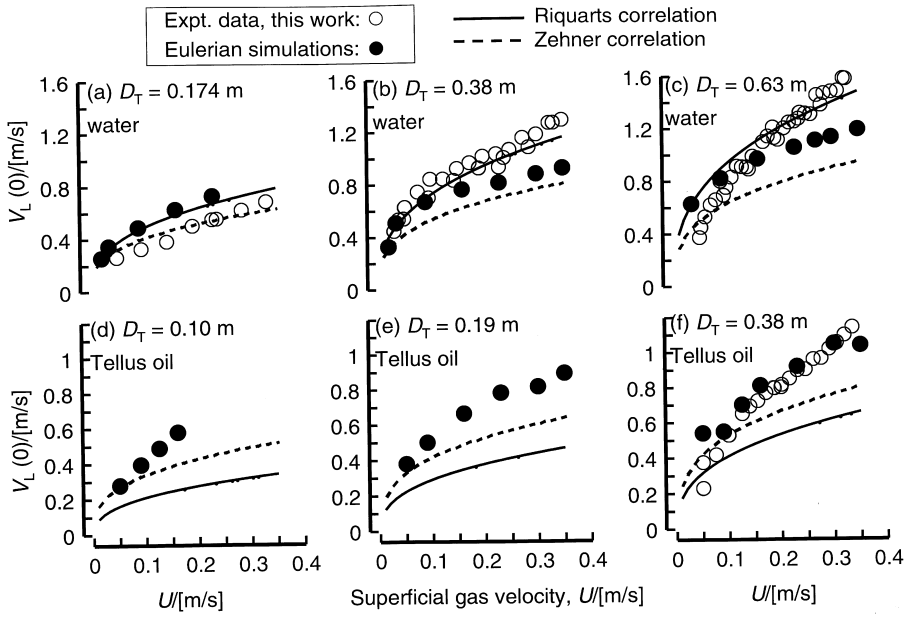

Fig. 10. Comparison of experimental values of centre-line velocity $V_L(0)$ with 2D Eulerian simulations. Also shown for comparison purposes are the Riquarts (1981) and Zehner (1986) correlations.

5. Conclusions

The following major conclusions can be drawn from the present work.

1. For reasonable predictions of radial distribution of liquid velocity and gas hold-up we must resort to complete three-dimensional Eulerian simulations.

2. For estimation of average gas hold-ups in the dispersion and circulating liquid velocities, typified by the centre-line velocity $V_L(0)$, two-dimensional simulations assuming cylindrical axi-symmetry are of adequate accuracy.

3. On the basis of the comparison of Eulerian simulations with experimental data obtained in columns of diameters ranging from 0.1 to 0.63 m, we conclude that

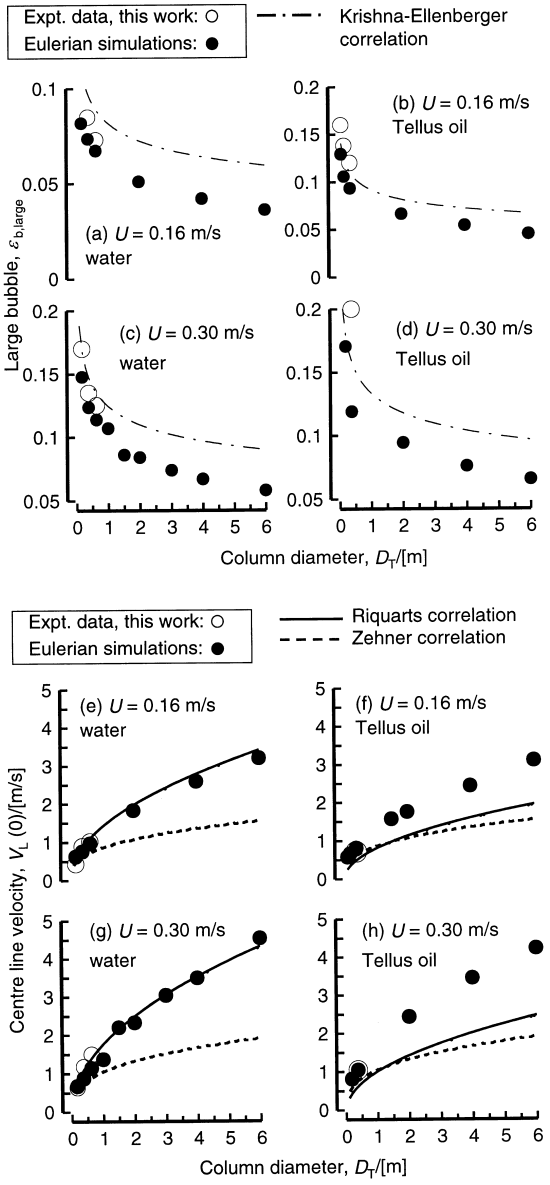

Fig. 11. (a)–(d). Influence of column diameter on large bubble hold-up for air–water and air–Tellus oil systems. Also shown is the correlation of Krishna and Ellenberger (1996) correlation; (e)–(h). Influence of column diameter on centre-line velocity $V_L(0)$ air–water and air–Tellus oil systems. Also shown are the extrapolation trends for $V_L(0)$ using the Riquarts (1981) and Zehner (1986) correlations.

the simulations reflect the correct trends with scale and liquid properties; see Figs. 9 and 10.

4. Eulerian simulations of the scale dependence of the centre-line $V_L(0)$ shows that these velocities can approach values of about 4–5 m/s when the column diameter is increased to 6 m. The simulations further show that the liquid viscosity has practically no effect on $V_L(0)$. On the basis of the Eulerian simulations we are able to recommend the use of the Riquarts correlation (7) provided we use the kinematic viscosity of water for all systems.

5. The strong increase in $V_L(0)$ with scale has the effect of accelerating the gas bubbles leading to significant reduction in the gas hold-up; this is underlined in the simulation results of Fig. 11(a)–(d). The reduction in hold-up is significantly stronger than that anticipated by the Krishna and Ellenberger (1996) correlation. Experimental data in the literature on gas hold-up and $V_L(0)$ in the churn-turbulent regime are restricted to columns smaller than 1 m in diameter and therefore there is a need for experimental verification with larger column diameters in order to verify the strong scale dependence anticipated by the Eulerian simulations.

Acknowledgements

The Netherlands Organisation for Scientific Research (NWO) is gratefully acknowledged for providing financial assistance to J.M. van Baten.

References

Akita, K., & Yoshida, Y. (1973). Gas hold-up and volumetric mass-transfer coefficient in bubble columns. *Industrial and Engineering Chemistry, Process Design and Development*, *12*, 76–80.

Bach, H. F., & Pilhofer, T. (1978). Variation of gas hold-up in bubble columns with physical properties of liquids and operating parameters of columns. *German Chemical Engineering*, *1*, 270–275.

Bauer, M., & Eigenberger, G. (1999). A concept for multi-scale modeling of bubble columns and loop reactors. *Chemical Engineering Science*, *54*, 5109–5117.

Bernemann, K. (1989). *Zur Fluiddynamik und zum Vermischungsverhalten der flüssigen Phase in Blasensäulen mit längsangeströmten Rohrbundeln*. Ph.D. thesis, University Dortmund.

Boisson, N., & Malin, M. R. (1996). Numerical prediction of two-phase flow in bubble columns. *International Journal of Numerical Methods in Fluids*, *23*, 1289–1310.

Clift, R., Grace, J. R., & Weber, M. E. (1978). *Bubbles, drops and particles*. San Diego: Academic Press.

Collins, R. (1967). The effect of a containing cylindrical boundary on the velocity of a large gas bubble in a liquid. *Journal of Fluid Mechanics*, *28*, 97–112.

Deckwer, W. D. (1992). *Bubble column reactors*. New York: Wiley.

De Swart, J. W. A., Van Vliet, R. E., & Krishna, R. (1996). Size, structure and dynamics of "large" bubbles in a 2-D slurry bubble column. *Chemical Engineering Science*, *51*, 4619–4629.

Ellenberger, J., & Krishna, R. (1994). A unified approach to the scaleup of gas solid fluidized and gas-liquid bubble column reactors. *Chemical Engineering Science*, *49*, 5391–5411.

Fan, L. S., & Tsuchiya, K. (1990). *Bubble wake dynamics in liquids and liquid–solid suspensions*. Boston: Butterworth-Heinemann.

Grevskott, S., Sannæs, B. H., Dudukovic, M. P., Hjarbo, K. W., & Svendsen, H. F. (1996). Liquid circulation, bubble size distributions, and solids movement in two- and three-phase bubble columns. *Chemical Engineering Science*, *51*, 1703–1713.

Grienberger, J., & Hofmann, H. (1992). Investigations and modelling of bubble columns. *Chemical Engineering Science*, *47*, 2215–2220.

Harmathy, T. J. (1960). Velocity of large drops and bubbles in media of infinite or restricted extent. *A.I.Ch.E. Journal*, *6*, 281–288.

Hikita, H., Asai, S., Tanigawa, K., & Kitao, M. (1980). Gas hold-up in bubble columns. *Chemical Engineering Journal*, *20*, 59–67.

Hills, J. H. (1974). Radial non-uniformity of velocity and voidage in a bubble column. *Transactions of the Institution of Chemical Engineers*, *52*, 1–9.

Hughmark, G. A. (1967). Hold-up and mass transfer in bubble columns. *Industrial and Engineering Chemistry, Process Design and Development*, *6*, 218–220.

Jakobsen, H. A., Sannæs, B. H., Grevskott, S., & Svendsen, H. F. (1997). Modeling of bubble driven vertical flows. *Industrial and Engineering Chemical Research*, *36*, 4052–4074.

Joshi, J. B. (1980). Axial mixing in multiphase contactors — a unified correlation. *Transactions of the Institution of Chemical Engineers*, *58*, 155–165.

Kawase, Y., & Moo-Young, M. (1989). Turbulent intensity in bubble column. *Chemical Engineering Journal*, *40*, 55–58.

Krishna, R., & Ellenberger, J. (1996). Gas hold-up in bubble column reactors operating in the churn-turbulent flow regime. *A.I.Ch.E. Journal*, *42*, 2627–2634.

Krishna, R., Ellenberger, J., & Sie, S. T. (1996). Reactor development for conversion of natural gas to liquid fuels: A scale up strategy relying on hydrodynamic analogies. *Chemical Engineering Science*, *51*, 2041–2050.

Krishna, R., Van Baten, J. M., & Ellenberger, J. (1998). Scale effects in fluidized multiphase reactors. *Powder Technology*, *100*, 137–146.

Krishna, R., & Van Baten, J. M. (1999). Simulating the motion of gas bubbles in a liquid. *Nature*, *398*, 208.

Krishna, R., Urseanu, M. I., van Baten, J. M., & Ellenberger, J. (1999a). Rise velocity of a swarm of large gas bubbles in liquids. *Chemical Engineering Science*, *54*, 171–183.

Krishna, R., Urseanu, M. I., van Baten, J. M., & Ellenberger, J. (1999b). Influence of scale on the hydrodynamics of bubble columns operating in the churn-turbulent regime: Experiments vs Eulerian simulations. *Chemical Engineering Science*, *54*, 4903–4911.

Kumar, S., Vanderheyden, W. B., Devanathan, N., Padial, N. T., Dudukovic, M. P., & Kashiwa, B. A. (1995). Numerical simulation and experimental verification of gas–liquid flow in bubble columns. In *Industrial mixing fundamentals with applications*, *A.I.Ch.E. Symposium Series No. 305*, vol 91 (pp. 11–19).

Lapin, A., & Lübbert, A. (1994). Numerical simulation of the dynamics of two-phase gas–liquid flows in bubble columns. *Chemical Engineering Science*, *49*, 3661–3674.

Nottenkämper, R., Steiff, A., & Weinspach, P. M. (1983). Experimental investigation of hydrodynamics of bubble columns. *German Chemical Engineering*, *6*, 147–155.

Ohki, Y., & Inoue, H. (1970). Longitudinal mixing of the liquid phase in bubble columns. *Chemical Engineering Science*, *25*, 1–16.

Reilly, I. G., Scott, D. S., De Bruijn, T. J. W., Jain, A. K., & Piskorz, J. (1986). A correlation for gas hold-up in turbulent bubble column. *Canadian Journal of Chemical Engineering*, *64*, 705–717.

Reilly, I. G., Scott, D. S., De Bruijn, T. J. W., & MacIntyre, D. (1994). The role of gas phase momentum in determining gas hold-up and hydrodynamic flow regimes in bubble column operations. *Canadian Journal of Chemical Engineering*, *72*, 3–12.

Rhie, C. M., & Chow, W. L. (1983). Numerical study of the turbulent flow past an airfoil with trailing edge separation. *AIAA Journal*, *21*, 1525–1532.

Riquarts, H. P. (1981). Strömungsprofile, Impulsaustausch und Durchmischung der flüssigen Phase in Bläsensaulen. *Chemie Ingenieur Technik*, *53*, 60–61.

Sanyal, J., Vasquez, S., Roy, S., & Dudukovic, M. P. (1999). Numerical simulation of gas–liquid dynamics in cylindrical bubble column reactors. *Chemical Engineering Science*, *54*, 5071–5083.

Sokolichin, A., & Eigenberger, G. (1994). Gas–liquid flow in bubble columns and loop reactors: Part I. Detailed modelling and numerical simulation. *Chemical Engineering Science*, *49*, 5735–5746.

Sokolichin, A., & Eigenberger, G. (1999). Applicability of the standard — turbulence model to the dynamic simulation of bubble columns: Part I. Detailed numerical simulations. *Chemical Engineering Science*, *54*, 2273–2284.

Torvik, R., & Svendsen, H. F. (1990). Modelling of slurry reactors. A fundamental approach. *Chemical Engineering Science*, *45*, 2325–2332.

Ueyama, K., & Miyauchi, T. (1979). Properties of recirculating turbulent two phase flow in gas bubble columns. *A.I.Ch.E. Journal*, *25*, 258–266.

Ulbrecht, J. J., Kawase, Y., & Auyeung, K. F. (1985). More on mixing of viscous liquids in bubble columns. *Chemical Engineering and Communication*, *35*, 175–191.

Van Doormal, J., & Raithby, G. D. (1984). Enhancement of the SIMPLE method for predicting incompressible flows. *Numerical Heat Transfer*, *7*, 147–163.

Vermeer, D. J., & Krishna, R. (1981). Hydrodynamics and mass transfer in bubble columns operating in the churn-turbulent regime. *Industrial and Engineering Chemistry. Process Design and Development*, *20*, 475–482.

Wilkinson, P. M., Spek, A. P., & Van Dierendonck, L. L. (1992). Design parameters estimation for scale-up of high-pressure bubble columns. *A.I.Ch.E. Journal*, *38*, 544–554.

Zehner, P. (1986). Momentum, mass and heat transfer in bubble columns. Part 1. Flow model of the bubble column and liquid velocities. *International Chemical Engineering*, *26*, 22–35.